The 'nanobig rods' class of gold nanorods: optimized dimensions for improved *in vivo* therapeutic and imaging efficacy

Constantin Ungureanu[1,†], Gerben A. Koning,[2] Ton G. van Leeuwen[1,3] and Srirang Manohar[1‡]

[1]Biomedical Photonic and Imaging Group, MIRA Institute for Biomedical Technology and Technical Medicine, Faculty of Science and Technology, University of Twente, P.O. Box 217, 7500AE Enschede, The Netherlands

[2]Laboratory Experimental Surgical Oncology, Section Surgical Oncology, Department of Surgery, Erasmus Medical Center, Rotterdam, The Netherlands

[3]Biomedical Engineering and Physics, Academic Medical Center, University of Amsterdam, PO Box 22700, 1100 DE Amsterdam, The Netherlands

Abstract.

Currently, gold nanorods can be synthesized in a wide range of sizes. However, for intended biological applications gold nanorods with approximate dimensions 50nm x 15nm are used. We investigate by computer simulation the effect of particle dimensions on the optical and thermal properties in the context of the specific applications of photoacoustic imaging. In addition we discuss the influence of particle size in overcoming the following biophysical barriers when administrated *in vivo*: extravasation, avoidance of uptake by organs of the reticuloendothelial system, penetration through the interstitium, binding capability and uptake by the target cells. Although more complex biological influences can be introduced in future analysis, the present work illustrates that larger gold nanorods, designated by us as "nanobig rods", may perform relatively better at meeting the requirements for successful *in vivo* applications compared to their smaller counterparts which are conventionally used.

† *c.ungureanu@tue.nl.*

‡ *s.manohar@utwente.nl.*

1. Introduction

One of the most important property of gold nanoparticles (AuNP) is the intense absorption of light at specific wavelengths, due to the phenomenon of localized surface plasmon resonance (LSPR). Additionally, these particles are relatively biological inert and by using different conjugation strategies, such as PEGylation [1, 2, 3], where antibodies are attached on their surface, they can be used to target specific biomolecules.

SPR occurs when light of a specific frequency sets free electrons of the AuNP surface into collective resonant oscillations (plasmons). The resonant frequency is uniquely defined by particle size, shape [4, 5, 6] and dielectric enviroment. At resonance, the interaction of the incident light and the AuNP is high, leading to narrow absorption and/or scattering peaks in the spectra. In asymmetric AuNP, plasmons can be created along the different axes of the particle, giving rise to multiple plasmon bands in the spectra. For example in gold nanorods (AuNR) [7, 8], resonant oscillations can occur along the short axis and the long axis, causing a transverse peak (TP) and a longitudinal peak (LP) respectively in the spectra. The TP is situated in the green region of the spectrum; the LP is red-shifted and tunable with aspect ratio [4] to occur in near infrared region (NIR). The NIR wavelength region is interesting for applications in tissue, since absorption (μ_a) and scattering (μ_s) coefficients of tissue are relatively low in this region, allowing high penetration of light for imaging into tissue (higher than 1 cm) [9, 10, 11]. Since the LP-driven absorption peak of AuNRs occurs in the NIR, these particles can be used as imaging contrast agents especially in photoacoustic imaging [12, 13, 14, 15, 16, 17].

Under illumination conditions of thermal and stress confinement, the local temperature rise produces ultrasound waves by photoacoustic effect; measurement of the ultrasound transients allows detection and visualization of the disease site. The temperature rise around irradiated particles can also produce therapeutic effects. CW (continous wave) light irradiation can be used to cause cell death in the process of hyperthermia [18, 19, 4, 20].

For these biomedical applications, various methods have been researched in pre-clinical studies whereby the NPs can be functionalized [21] by conjugating them with antibodies, thereby imparting them with the capability to target disease sites such as cancer [22, 12].

The ability to detect the disease or to affect a complete therapeutic action is dependent on the extent of interaction that the NPs will have with light, phenomenon for which NPs can be tailored by appropriate choice of physical features such as size and aspect ratio. Also important, is extent to which a therapeutically relevant concentration accumulates homogeneously throughout the disease area. This requires design of physical and biochemical features of the NPs, which calls for some understanding of the physiology in normal and tumor tissue, and in their respective vasculature.

In general, for biomedical application of NPs the following steps are required for deployment of NPs for diagnostic or therapeutic purposes.

(i) synthesis of the NPs
(ii) NP bioconjugation with disease specific antibodies (mAb)
(iii) topical or systemic administration of mAb-NPs
(iv) circulation in blood stream
(v) extravasation at disease site through leaky vasculature
(vi) transport in tumor
(vii) binding to the targeted cells
(viii) triggering of NPs present at the diseased site (tumor) with light, for detection or therapy.

Currently AuNRs can be synthesized with large variations in physical dimensions (length, width and aspect ratio) each variant having specific optical properties [6]. Typically, the entire "optical diagnostic and therapeutic window"in the NIR spectrum can be covered by AuNRs with aspect ratios (a.r) ranging from 2.5 to 5, and effective radii (r_{eff}) from 5 nm to 35 nm [23, 7, 6]. The r_{eff} of a AuNR is the radius of a sphere having the same volume as the particle [24].

The immediate question is: which particle among these are optimum for diagnostic and/or therapeutic purposes? The goal of this article is to provide a possible solution to this problem.

Using computer simulations and analysis of data reported in literature, we find that larger AuNRs (larger r_{eff}), while still preserving appropriate a.r, can largely meet the requirements for successful use in biological applications. These particles designated by us "nanobig rods" have better physical, optical and thermal properties compared with the commonly used gold nanorods which have r_{eff} smaller than half of mean free path of electrons in gold. Next to the improved optical responses, we also consider the effects of particle dimensions can have on *in vivo* behavior such as on extravasation, uptake by cells and thermal stability in laser field.

Materials and methods

Simulation of optical properties of AuNRs

The DDSCAT 6.1 [24] package (an implementation of the Discrete Dipole Approximation method) was used to simulate the optical properties of AuNRs. The method discretizes a particle into dipoles, and the electromagnetic field scattered by the nanoparticle is calculated taking into account dipole-dipole and dipole-light interaction. The approach allows the interaction of light with arbitrary shaped particles to be modeled and simulated, with a knowledge of parameters such as the dielectric function of the material, refractive index of media and particle orientation relative to incident electromagnetic field. For simulating AuNR, we used the dielectric function of bulk gold [25], and water with refractive index of 1.33 was considered as embedding medium [8].

Criteria for choosing sizes of the gold nanorods

Optical properties

In *in vivo* biomedical applications collections of particles are involved. The absorption coefficient μ_a [9] of such an ensemble is wavelength dependent [26] and is calculated as the product of particle concentration (N) and absorption cross-section (C_{abs}) of the particle ($\mu_a = N \times C_{abs}$) where:

$$C_{abs} = \pi r_{eff}^2 Q_{abs} \tag{1}$$

with Q_{abs} the absorption efficiency of the particle. For maximizing light interactions with the NRs embedded in tissue, the following requirements for the NR need to be fulfilled:

- the LP peak has to be located in the NIR spectral region where background tissue optical properties, μ_a and μ_s, are lower than in visible range [27, 28],
- the optical interaction coefficients, μ_a or μ_s, should be as high as possible, to increase the light induced effect necessary for detection or therapy.

AuNRs are currently synthesized using various modifications [6] to a seed-mediated silver-assisted growth protocol [29] resulting in variously sized rods. We modelled a wide range of AuNRs with r_{eff} (5-35 nm) and aspect ratios (AR) (2.5 - 4) to include these different particles.

For *in vivo* optical imaging and photothermal applications, 800 nm is a wavelength that is typically used [9, 30]. In this NIR region, tissue has relatively low μ_a and μ_s Further, sources of 800 nm in the ns regime by pumping OPO crystals are readily available for photoacoustic imaging. CW laser sources with emission wavelength at 800 nm are also reported in studies about hyperthermic effect [31, 32]. For these reasons we make comparisons between AuNRs which show their LP peaks around this wavelength.

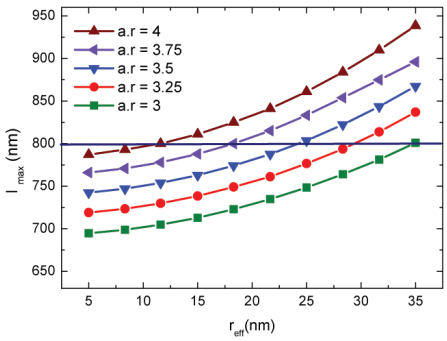

Figure 1. Location of the longitudinal plasmon (LP) peaks simulated for AuNRs with aspect ratios (AR) 3, 3.25, 3.5, 3.75 and 4, as a function of effective radius.

Figure 1 shows as a function of r_{eff} the spectral locations of the LP absorption peaks for AuNRs with AR 3, 3.25, 3.5, 3.75 and 4. As observed earlier [33], not only the AR but also the volume of the NR determines the position of the LP peak. The LP

peaks red-shift with increasing r_{eff}, but the region around 800 nm is covered only by AuNRs with AR between 3 and 4, possessing r_{eff} between 11 and 35 nm.

The values of simulated absorption (Q_{abs}) and scattering (Q_{sca}) efficiencies at the LP peaks for a.r 3 to 4 as a function of r_{eff} are shown in figure 2 (a) and (b). Irrespective of a.r, Q_{abs} values have a peak around $r_{eff} = 17.5$ nm. The diameter of such particle is close to the mean free path of electrons in gold ($\approx$ 42nm [34]).

Q_{sca} increases with increasing r_{eff} but NRs with $r_{eff} < 10$ nm can be considered pure absorbers as Q_{sca} is negligible in comparison with Q_{abs}. For $r_{eff} > 27$ nm (see figure 2), scattering is larger than absorption. This is the consequence of radiation damping effects which occur in larger particles [35], a behavior also seen in gold nanospheres [36].

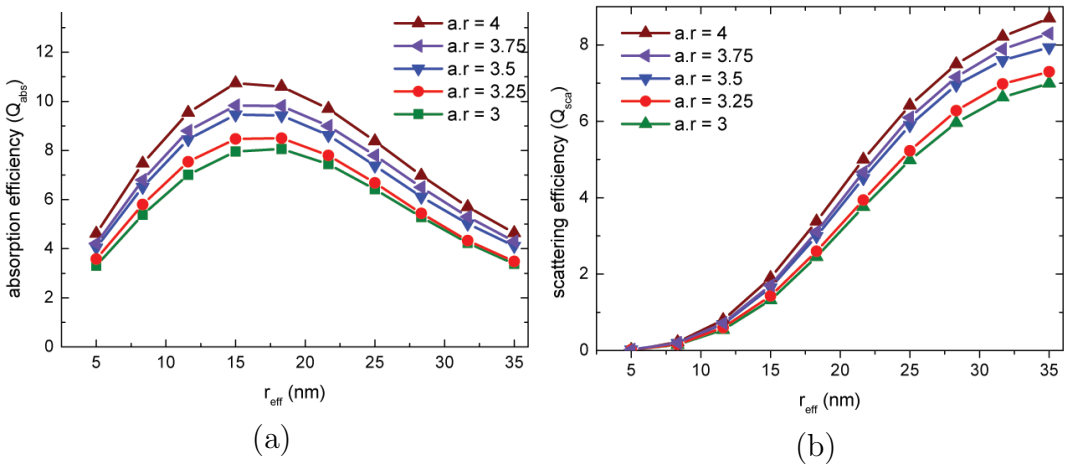

(a) (b)

Figure 2. Simulated absorption efficiency Q_{abs} (a), and scattering efficiency Q_{sca} (b), at the LP as a function of effective radius for aspect ratios from 3.0 to 4. Q_{abs} passes though a maximum at about 17.5 nm. Q_{sca} increases with effective radius reaching saturation levels above 35 nm.

Figure 3 depicts the optical properties in the form of Q_{abs} and Q_{sca} values at 800 nm for particles with a.r between 3 and 4, and r_{eff} between 11 and 35 nm. From figure 3(a) we can identify an optimal combination of a.r= 3.75 and r_{eff} =17.5 nm for obtaining the LP peak at 800 nm with the highest Q_{abs}. As shown above, for thermal response upon irradiation, μ_a is the most important parameter.

We calculated further the μ_a for solutions containing particles simulated in figure 1, using the Q_{abs} and Q_{sca} from figure 3 at the same particle concentration (10^9/ml). The result displayed in figure 4 shows that collections of particles with the combination of a.r of 3.75 and r_{eff} =17.5 nm are not actually optimal, with particles with a.r of 3.5 and r_{eff} =25 nm possessing higher μ_a and μ_s. It can be observed that increasing the r_{eff} and decreasing the a.r will not increase μ_a. The geometrical cross section in this case will not counterbalance sufficient lower Q_{abs}. Particles with a.r= 3 and r_{eff} =35 nm may be used for example only in scattering based detection systems.

Thus, from the optical imaging or photothermal perspective, larger AuNRs are more favorable than the commonly used smaller AuNRs.

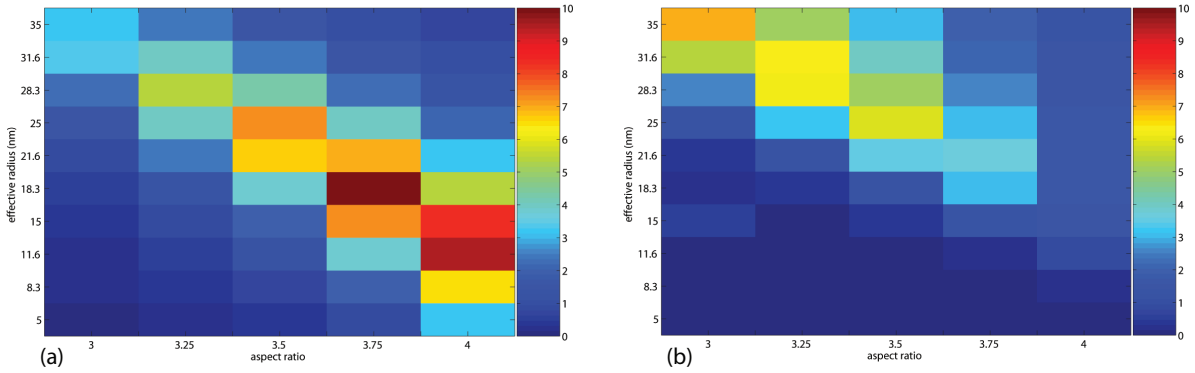

Figure 3. Simulated absorption efficiency (a) Q_{abs}, and scattering efficiency (b) Q_{sca}, at 800 nm as functions of effective radii (r_{eff}) and aspect ratios (a.r).

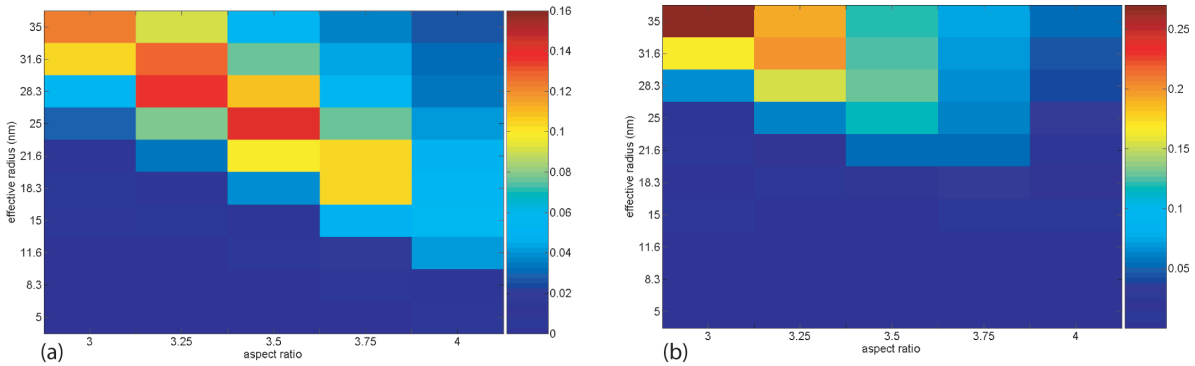

Figure 4. Simulated absorption coefficient μ_a (cm^{-1}) (a) and scattering coefficient μ_s (cm^{-1}) (b) calculated at 800 nm for a collection of 10^9/ml rods as a function of r_{eff} and a.r at 800 nm.

The length and width of this AuNR assuming a hemispherically capped cylinder geometry is 100 nm and 28.5 nm respectively. We qualify these particles as "nanobig rods" for a clear identification further in discussion. We also name AuNRs with r_{eff} smaller than 17.5 nm as being "nanosmall rods" for differentiation in the discussion. As a thumb rule we define the "nanobig rods" as being those AuNRs with r_{eff} greater than half of the mean free path of electrons in gold.

Table 1. Actual dimensions of gold nanorods occupying the classes "nanosmall rods" and "nanobig rods" with aspect ratios and effective volumes that provide plasmon peaks at 800 nm.

r_{eff}	a.r	length (nm)	width(nm)	size class
11	4.0	50	12.5	"nanosmall rods"
24	3.5	100	28.5	"nanobig rods"

We will further compare the commonly used "nanosmall rods" with the proposed "nanobig rods". The dimensions of these particles are summarized in Table 1.

Circulation in the blood, extravasation and interstitial penetration

1.0.1. Circulation of AuNR in blood Upon intravenous administration of AuNRs, the particles are distributed *via* the vascular system to various organs and tissues in the body. During this transport, the AuNRs interact with various blood components such as cells and proteins. Nanoparticles coated with hydrophilic, neutral polymers such as PEG, possess relative stealth properties in the blood [37]. The steric stabilization of the particles with the polymers prevents or minimizes adsorption of proteins such as opsonin ligands, which could otherwise interact with macrophage cell receptors and thereby mark a particle for uptake. We have recently shown that PEGylation of AuNR prolongs the blood circulation half-life of the particles to 19 hours, while the non-PEG AuNR are trapped rapidly within minutes in the liver and spleen [38, 1].

Particles can be bioconjugated with specific antibodies to attach to targeted cells. However, it has been shown that the presence of antibodies on the surface of particles increases their chances of being recognized and engulfed by macrophages in the RES (Reticulo Endothelial System)[39, 40]. It was also shown that the uptake level of bioconjugated nanoparticles by macrophages is proportional with loading of antibodies on the surface [41]. Only at low densities of antibody coverage, sufficient target binding to tumor cells can be achieved while maintaining minimal macrophage interaction.

At this point, there is no literature comparing RES uptake of AuNR of various sizes; most studies have used the "nanosmall rods" particles (65x11nm [37], 50 x15 nm [42], 56x13 nm[43]).

Another issue with smaller nanoparticles represents their capacity to cross the Brain Blood Barrier (BBB). This phenomen is not desired if not specifically targeted. As discussed in recent publications [44, 45, 46, 47] particles smaller than 20 nm can cross the BBB and can be found also in retinal layers. Larger particles such as "nanobig rods" (width $>$ 20 nm) will have lower probability to cross the BBB.

In the spleen, studies have shown that particles between 100 and 150 nm are more efficiently filtered by the splenic bed [48]. At this moment there is insufficient data to present clear evidence for the preference of "nanosmall rods" or "nanobig rods" particles in this context.

1.0.2. Extravasation Unlike normal vasculature, angiogenic blood vessels associated with carcinoma, are in general poorly organized with chaotic branching and are dilated, tortuous and leaky. The vessels can have gaps as large as 10 μm between endothelial cells [49, 50, 51]. Moreover, fenestration sizes vary from patient to patient, dependence on the type of cancer and change over time.

Solid tumors have interstitial hypertension which reduces the convection of the particles across the vessel walls. The progressively higher pressures from the periphery

to the center of of the tumor are due to the proliferation of cancer cells and impaired lymphatics. For the NRs to infiltrate the tumor, the particles will have to traverse this fluid interspersed cross-linked network of collagen and elastin fibers [49, 52]. Movement in this region is by diffusion and convection, however convective transport progressively reduces towards the center of the tumor due to the elevated pressures.

Experimental studies using 90 nm liposomes have shown that these could penetrate only distances of 10-20 μm from the microvasculature in mice, forming relatively static perivascular clusters [53]. It has been estimated that such large particles could take months to traverse 1 mm of tumor tissue, while smaller structures such as an IgG molecule with a hydrodynamic radius of 5 nm would take a considerably lower 2-3 days [54]. Thus, it is evident that smaller sizes of the NRs will be favorable for interstitial penetration. Data presented in literature on extravasation of nanoparticles shows that larger particles tend to remain localized at the vascular bed and do not extravasate deep into tumor[41]. This could make the case against "nanobig rods" , since the spatial heterogeneity of particle distribution in tumors can affect the visualization of tumors by photoacoustic methods by not revealing the entire tumoral volume. However, their presence at the tumor periphery can provide indications about the tumor size.

1.0.3. Uptake by Target Cells When mAB-AuNRs interact with the target cells, they can be taken up by the cells *via* receptor-mediated endocytosis (RME) [55, 56]. This process is initialized by clathrin, a cytoplasmic protein which assists the formation of a vesicle around the particles, through invagination of the plasma membrane. The vesicle, or early endosome, is transported further to fuse with a lysosome where the constituents are degraded and ultimately excreted. This process can be fast and it usually takes less than an hour for a particle to cross the membrane and to arrive in the lysosome [57]. A high surface area of the particle can help the internalization process, firstly by increasing the amount of antibodies that can be loaded on their surface, and secondly by increasing the area projected on the surface of the cell and thus the adhesion force as discussed in [58, 59, 60, 61]. The internalization process is desirable in some therapeutic applications because the drug molecules attached on their surface can be released in cytoplasmic space [62]. Another reason is that the temperature fields generated by the particle during laser irradiation can be confined in intracellular spaces localizing the affected area close to the nucleus or other important cellular organelles [63]. However, experiments in microsurgery using pulsed lasers have shown that the damage to cells produced by explosion, cavitation or bubble formation is limited to the targeted cells [64, 65, 66]. For larger tumors, where not all the cells contain AuNR this type of therapy will not be successful to eradicate the tumor. However, drug delivery can be still achieved *in vivo* by short pulsed lasers [67, 68] by cleaving the bond between the drug molecule and gold nanoparticle.

Chitrani *et al* [55] showed that shorter aspect ratios AuNRs with higher effective radii are internalized in greater numbers than longer aspect ratio NRs, which is supported by studies by Decuzzi and Ferrari [60]. In exocytosis (the excretion of foreign

bodies by the cells), the trend is reversed as the fraction of exocytosed particles is higher for higher aspect ratio AuNRs. Consequently, shorter aspect ratio NRs can stay longer in cells. Moreover, the optimum radius of spherical nanoparticles for internalization was found to be around 25 nm, both from experiment [55, 69] and theory [70, 71]. New reports [41] show that this optimum size actually is larger than 25 nm. This suggests that the "nanobig rods" with an effective radius around 24 nm and a shorter aspect ratio of 3.5 possess a higher propensity for cellular internalization than the conventional "nanosmall rods".

However, in the case of AuNR the internalization may not be desired because particles once engulfed tend to form large aggregated structures [72]. This situation will bring particles into plasmonic interaction range causing LP peaks to shift and broader depending on structure of the cluster.

Thermal response during pulsed laser irradiation

Pulsed lasers can induce larger temperatures in nanoparticles because heat will accumulate faster than losses across the surfaces. The temperature rise of the particles can be sufficient to cause vaporization of surrounding water/tissue layers [73, 65, 74]. When particle concentrations are high enough, bubble formation and subsequent collapse can cause damage to cells. With high laser intensities, the temperature rise can be so high that reshaping of the NRs into shorter NRs and into spheres may occur. The melting and/or fragmentation [75, 76] causes a drastic change in the optical properties, with the disappearance of the LP peak in an ensemble collection of irradiated AuNRs.

The stability of the NRs in laser field depends on the melting point of the particles, which in turns depends on their size and coating [77]. The energy (Q_m) and temperature required (T_m) for melting of AuNRs can be calculated using [77, 78]:

$$Q_m = \rho V(c_p[T_{NR} - T_0) + \Delta H_f] \tag{2}$$

$$T_{NR} = T_b(1 - 6\frac{rS}{8\pi r_{eff}^3}) \tag{3}$$

where ρ is bulk density (19300 kg m^{-3}), c_p is heat capacity (129 J kg^{-1} K^{-1}), ΔH_f is enthalpy of fusion(6.5×10^4 J kg^{-1}), T_b is the bulk melting temperature (1330 K), T_0 (310K) is the initial temperature, T_{NR} is the nanoparticle melting temperature and r is the atomic radius (135 pm) of gold. V is the volume and S the surface area of the AuNR before melting. Equation 3 accounts for the shape factor and for the cohesive energy of the metallic particle [78].

Using these equations, we obtain melting temperatures for "nanosmall rods" as 1281 K, and for "nanobig rods" as 1307 K. As expected, the smaller particle possesses a lower temperature for melting. The calculated energy (equation 2) required to completely reshape "nanobig rods" and "nanosmall rods" into spheres is 215 fJ and 20 fJ, respectively. Thus "nanobig rods" particles are more resistant to reshaping and can support higher laser powers, making them better suited for use as contrast agents in photoacoustic imaging.

Availability of synthetic methods

The final criterion for the choice of nanoparticle dimensions is whether the particles can be synthesized. The most well established protocol, in terms of yield, monodispersity and fine control of aspect ratio is the silver assisted seed-mediated method of Nikoobakht and El-Sayed [29, 79] that requires the addition of gold seed to a growth solution with shape/size directing surfactant CTAB and silver nitrate. Using different $AgNO_3$ concentrations in the growth solution allows excellent tuning of the a.r of the NRs, but only to a maximum of around 4. In general these AuNRs fall under the "nanobig rods" class (see Table 2).

The method to grow AuNR using wet chemistry methods had actually been pioneered by the Murphy group [80], but their method did not use silver. Gold seed are made to initiate nanocrystal growth in growth solutions with CTAB with slow controlled reduction. The groups of Liz-Marzan and Mulvaney [81] showed that temperature, CTAB concentrations, amount and sizes of the gold seed and decrease in the reaction rate allows good control over the sizes and a.r of the particles. Further studies [82, 83] also showed that the a.r could be made to increase monotonously in size throughout the growth process, which is not observed when silver is present during reduction. Further the sizes of the particles are larger than those which use the silver -assisted aproach and can be described as "nanobig rods" NRs (see Table 2).

Table 2. Typical sizes of AuNR synthesizable with different protocols

reference	length (nm)	width(nm)	effective radius (nm)	aspect ratio	position of LP (nm)	class
[84]	10-30	5-10	4-8	2.2-4	670-790	"nanosmall rods"
[85]	41-52	14-20	11-15	2.3-3.6	675-850	"nanosmall rods"
[81]	52-187	20-30	15-34	2.2-6.7	724-1080	"nanobig rods"

It should be admitted that methods which do not use silver result in large amounts of spheres as byproducts. However, efficient separation of AuNR from mixtures of nanorods and nanospheres can be performed using centrifugation utilizing shape-dependent sedimentation behavior [86].

Concluding remarks

We have identified a size class, "nanobig rods", which has several advantages compared to their smaller counterparts, "nanosmall rods", which are used conventionally. The discussed performance of these two size classes for various features is summarized in Table 3.

Table 3. Performance of the two NR classes in the selection criteria

Feature	"nanobig rods"	"nanosmall rods"
LP at 800 nm	+	+
C_{abs} at LP peak	++	+
C_{sca} at LP peak	++	+
Circulation in blood	?	?
extravasation at tumor	+	++
interstitium transport	+	++
target cell uptake	?	?
lower number for contrast effect	++	+
thermal stability	++	+
quality of synthesis	+	++

Some performance indicators can be conflicting and a judicious balance between the different criteria has to be found. The extent of mAb loading on a particle, which depends on the surface area, e.g. will improve the adhesion to the target cells. On the other hand, enhanced immunogenicity of the particle with more mAbs may increase uptake by the RES and thus lower the final dose arriving in the tumor. Moreover, as shown in[87], the bioconjugation improve the internalization rather than extravasation.

Finally, modulation of the microenvironment of the tumors may improve the uptake of the AuNRs. Some examples of vascular manipulation have been described to improve delivery of drugs and/or drug containing nano-carriers to solid tumors. Transient normalization [88] of the abnormal structure of tumor vasculature, is known to improve perfusion and thereby drug delivery. The use of vaso-dilatation factors [89], or normalization approaches that increase vascular permeability for instance by using growth factors or cytokines [50], or heat [90, 91] are known to increase accumulation and transport of NPs. A final approach of vascular manipulation is the approach that aims at lowering the interstitial hypertension using lytic enzymes[92, 49].

Additional experiments and theoretical calculations are necessary to show which among "nanobig rods" and "nanosmall rods" particles are better suited for biological applications. Techniques similar to Particle Swarm Optimization (PSO) [93] may be used to optimize the size of gold nanorods for biological applications. However, if we take into account only the optical and thermal properties, the "nanobig rods" particles have better properties for biological applications than "nanosmall rods" ones.

2. Acknowledgements

This work is funded through the thrust area program NIMTIK of the University of Twente; through the PRESMITT project (IPD067771) of the SenterNovem program IOP Photonic Devices; and by the Nederlandse Wetenschappelijk Organisatie (NWO)

and Stichting Technische Wetenschappen (STW) through project TTF 6527.

References

[1] Lankveld D P, Rayavarapu R G, Krystek P, Oomen A G, Verharen H W, van Leeuwen T G, de Jong W H and Manohar S 2011 Blood clearance and tissue distribution of pegylated and non-pegylated gold nanorods after intravenous administration in rats *Nanomedicine* **6** 339

[2] Jokerst J V, Lobovkina T, Zare R N and Gambhir S S 2011 Nanoparticle pegylation for imaging and therapy *Nanomedicine* **6(4)** 715728

[3] Green H N, Martyshkin D V, Rodenburg C M, Rosenthal E L and Mirov S B 2011 Gold nanorod bioconjugates for active tumor targeting and photothermal therapy *Journal of Nanotechnology* **2011** 1

[4] Huang X, Neretina S and El-Sayed M A 2009 Gold nanorods: From synthesis and properties to biological and biomedical applications *Adv Mater* **21** 4880

[5] Jain P K, Huang X, El-Sayed I H and El-Sayed M 2008 Noble metals on the nanoscale: Optical and photothermal properties and some applications in imaging, sensing, biology, and medicine *Acc. Chem. Res.* **41** 1578

[6] Perez-Juste J, Pastoriza-Santos I, Liz-Marzan L M and Mulvaney P 2005 Gold nanorods: Synthesis, characterization and applications *Coordination Chemistry Reviews* **249** 1870

[7] Prescott S W and Mulvaney P 2006 Gold nanorod extinction spectra *J. Appl. Phys* **99** 123504

[8] Ungureanu C, Rayavarapu R G, Manohar S and van Leeuwen T G 2009 Discrete dipole approximation simulations of gold nanorod optical properties: Choice of input parameters and comparison with experiment *J Appl Phys* **105** 102032

[9] Li C and Wang L V 2009 Photoacoustic tomography and sensing in biomedicine *Phys. Med. Biol* **54** 59

[10] Qin Z and Bischof J C 2012 Thermophysical and biological responses of gold nanoparticle laser heating *Chem. Soc. Rev.* **41,** 1191

[11] Yang X, Stein E W, Ashkenazi S and Wang L V 2009 Nanoparticles for photoacoustic imaging *WIREs Nanomed Nanobiotechnol* **1** 360368

[12] Manohar S, Ungureanu C and Leeuwen T G V 2011 Gold nanorods as molecular contrast agents in photoacoustic imaging: the promises and the caveats *Contrast Media & Molecular Imaging* **6(5)** 389

[13] Huang G, Yang S, Yuan Y and Xing D 2011 Combining x-ray and photoacoustics for in vivo tumor imaging with gold nanorods *Appl. Phys. Lett.* **99** 123701

[14] Su R, Liopo A, Ermilov S A, Brecht H P, Larin K and Oraevsky A A 2011 Optoacoustic tomography in preclinical research: in vivo distribution of highly purified peg-coated gold nanorods in *Proceedings of SPIE-OSA Biomedical Optics*

[15] Yeager D, Karpiouk A, Wang B, Amirian J, Sokolov K, Smalling R and Emelianov S 2012 Intravascular photoacoustic imaging of gold nanorod-labeled atherosclerotic plaques *Proc. SPIE 8223, Photons Plus Ultrasound: Imaging and Sensing* 82231Q–82231Q–7

[16] Mallidi S, Luke G P and Emelianov S 2011 Photoacoustic imaging in cancer detection, diagnosis, and treatment guidance *Trends Biotechnol* **29** 213

[17] Tong L, Wei Q, Wei A and Cheng J X 2009 Gold nanorods as contrast agents for biological imaging: Optical properties and surface conjugation and photothermal effects *Photochemistry and Photobiology* **85** 21

[18] Li M L, Wang J C, Schwartz J A, Gill-Sharp K L, Stoica G and Wang L V 2009 In-vivo photoacoustic microscopy of nanoshell extravasation from solid tumor vasculature *JBO Letters* **14** 010507

[19] Mallidi S, Larson T, Tam J, Joshi P P, Karpiouk A, Sokolov K and Emelianov S 2009 Multiwavelength photoacoustic imaging and plasmon resonance coupling of gold nanoparticles for selective detection of cancer *Nano Lett.* **9** 2825

[20] Oldenburg A L, Hansen M N, Ralston T S, Wei A and Boppart S A 2009 Imaging gold nanorods in excised human breast carcinoma by spectroscopic optical coherence tomography *J. Mater. Chem*

[21] Tiwari P M, Vig K, Dennis V A and Sin S R 2011 Functionalized gold nanoparticles and their biomedical applications *Nanomaterials* **1** 31

[22] Rayavarapu R, Petersen W, Ungureanu C, Post J, van Leeuwen T and Manohar S 2007 Synthesis and bioconjugation of gold nanoparticles as potential molecular probes for light-based imaging techniques *Int. J. Biomed. Imaging* **29817** 29817

[23] Harris N, Ford M J, Mulvaney P and Cortie M B 2008 Tunable infrared absorption by metal nanoparticles: The case for gold rods and shells *Gold Bulletin* **41** 5

[24] Draine B and Flatau P *2004, "User Guide to the Discrete Dipole Approximation Code DDSCAT 6.1", http://arxiv.org/abs/astro-ph/0409262v2.*

[25] Palik 1991 *Handbook of Optical Constants of Solids* Boston: Academic Press,

[26] Ungureanu C, Amelink A, Rayavarapu R G, Sterenborg H J C M, Manohar S and van Leeuwen T G 2010 Differential pathlength spectroscopy for the quantitation of optical properties of gold nanoparticles *ACS Nano* **4 (7)** 4081

[27] Vo-Dinh T 2002 *Biomedical Photonics Handbook.* Taylor & Francis,

[28] Franceschini M A, Gratton E, Hueber D M and Fantini S 1999 Near-infrared absorption and scattering spectra of tissues in vivo *Proc. SPIE* **3597**

[29] Nikoobakht B and El-Sayed M A 2003 Preparation and growth mechanism of gold nanorods (nrs) using seed-mediated growth method *Chem. Mater.* **15** 1957

[30] Dickerson E, Dreaden E, Huang X, El-Sayed I, Chu H, Pushpanketh S, McDonald J and El-Sayed M 2008 Gold nanorod assisted near-infrared plasmonic photothermal therapy (pptt) of squamous cell carcinoma in mice *Cancer Letters* **269** 57

[31] Choi W I, Kim J Y, Kang C, Byeon C C, Kim Y H and Tae G 2011 Tumor regression in vivo by photothermal therapy based on gold-nanorod-loaded, functional nanocarriers *ACS Nano* **5** 1995

[32] Cole J R, Mirin N A, Knight M W, Goodrich G P and Halas N J 2009 Photothermal efficiencies of nanoshells and nanorods for clinical therapeutic applications *J Phys Chem C* **113 (28)** 12090

[33] Jain P K, Lee K S, El-Sayed I H and El-Sayed M A 2006 Calculated absorption and scattering properties of gold nanoparticles of different size and shape and and composition: Applications in biological imaging and biomedicine *J Phys Chem B* **110 (14)** 7238

[34] Kooij E S and Poelsema B 2006 Shape and size effects in the optical properties of metallic nanorods *Phys. Chem. Chem. Phys* **8(28)** 3349

[35] Link S and El-Sayed M A 1999 Size and temperature dependence of the plasmon absorption of colloidal gold nanoparticles *J Phys Chem B* **103** 4212

[36] Yin G, Wang S Y, Xu M and Chen L Y 2006 Theoretical calculation of the optical properties of gold nanoparticles *J Koreean Phys Soc* **49** 2108

[37] Niidome T, Yamagata M, Okamoto Y, Akiyama Y, Takahashi H, Kawano T, Katayama Y and Niidome Y 2006 Peg-modified gold nanorods with a stealth character for in vivo applications *J. Control. Release* **114** 343

[38] von Maltzahn G, Park J H, Agrawal A, Bandaru N K, Das S K, Sailor M J and Bhatia S N 2009 Computationally guided photothermal tumor therapy using long-circulating gold nanorod antennas *Cancer Res* **69(9)** 38923900

[39] Koning G A, Morselt H W M, Gorter A, Allen T M, Zalipsky S, Scherphof G L and Kamps J A A M 2003 Interaction of differently designed immunoliposomes with colon cancer cells and kupffer cells. an in vitro comparison *Pharmaceut Res* **20** 1249

[40] Koning G A, Morselt H W M, Gorter A, Allen T M, Zalipsky S, Kamps J A A M and Scherphof G L 2001 Pharmacokinetics of differently designed immunoliposome formulations in rats with or without hepatic colon cancer metastases *Pharmaceut Res* **18** 1291

[41] Albanese A, Tang P S and Chan W C 2012 The effect of nanoparticle size, shape, and surface chemistry on biological systems *Annu. Rev. Biomed. Eng* **14** 1

[42] Kogan B, Andronova N, Khlebtsov N, Khlebtsov B, Rudoy V, Dementeva O, Sedykh E and Bannykh L 2008 Pharmacokinetic study of pegylated plasmon resonant gold nanoparticles in tumor-bearing mice *Technical Proceedings of the 2008 Nanotechnology Conference and Trade Show* **2** 65

[43] Wang L, Li Y F, Zhou L, Liu Y, Meng L, Zhang K, Wu X, Zhang L, Li B and Chen C 2010 Characterization of gold nanorods in vivo by integrated analytical techniques: their uptake, retention, and chemical forms *Anal. Bioanal. Chem.* **396** 1105

[44] Khlebtsov N and Dykman L 2011 Biodistribution and toxicity of engineered gold nanoparticles: a review of in vitro and in vivo studies *Chem. Soc. Rev.* **40** 1647

[45] Khlebtsov N G and Dykman L A 2011 Biodistribution and toxicity of gold nanoparticles *Nanotechnologies in Russia* **6** 17

[46] Terentyuk G S, Maslyakova G N, Suleymanova L V, Khlebtsov B N, Kogan B Y, Akchurin G G, Shantrocha A V, Maksimova I L, Khlebtsov N G and Tuchin V V 2009 Circulation and distribution of gold nanoparticles and induced alterations of tissue morphology at intravenous particle delivery *J. Biophotonics* **2** 292

[47] Zhao F, Zhao Y, Liu Y, Chang X, Chen C and Zhao Y 2011 Cellular uptake, intracellular trafficking, and cytotoxicity of nanomaterials *Small* **7** 1322

[48] Moghimi S, Porter C, Muir I S, Illum L and Davis S 1991 Non-phagocytic uptake of intravenously injected microspheres in rat spleen: influence of particle size and hydrophilic coating *Biochem Biophys Res Commun.* **177(2)** 861

[49] Jain R K 1998 Delivery of molecular and cellular medicine to solid tumours *J. Control. Release* **53** 49

[50] Seynhaeve A L, Hoving S, Schipper D, Vermeulen C E, aan de Wiel-Ambagtsheer G, van Tiel S T, Eggermont A M and ten Hagen T L 2007 Tumor necrosis factor mediates homogeneous distribution of liposomes in murine melanoma that contributes to a better tumor response *Cancer Res* **67(19)** 9455

[51] Koning G A and Krijger G C 2007 Targeted multifunctional lipid-based nanocarriers for image-guided drug delivery *Anti-Cancer Agents in Medicinal Chemistry* **16** 425

[52] Jain R K 1998 The next frontier of molecular medicine: Delivery of therapeutics *Nature Medicine* **4** 655

[53] Yuan F, Leunig M, Huang S K, Berk D A, Papahadjopoulos D and Jain R K 1994 Microvascular permeability and interstitial penetration of sterically stabilized (stealth) liposomes in a human tumor xenograft *Cancer Res* **54** 3352

[54] Kim K Y 2007 Nanotechnology platforms and physiological challenges for cancer therapeutics *Nanomed Nanotech Biol Med* **3** 103

[55] Chithrani B D and Chan W C W 2007 Elucidating the mechanism of cellular uptake and removal of protein-coated gold nanoparticles of different sizes and shapes *Nano Lett.* **7(6)** 1542

[56] Chithrani B D, Ghazani A A and Chan W C 2006 Determining the size and shape dependence of gold nanoparticle uptake into mammalian cells *Nano. Lett.* **6** 662

[57] Carmeliet P and Jain R K 2000 Angiogenesis in cancer and other diseases. *Nature* **407(6801)** 249

[58] Best J P, Yan Y and Caruso F 2012 The role of particle geometry and mechanics in the biological domain *Adv. Healthcare Mater* **1** 35

[59] Decuzzi P, Lee S, Decuzzi M and Ferrari M 2004 Adhesion of microfabricated particles on vascular endothelium: a parametric analysis. *Ann Biomed Eng* **32(6)** 793

[60] Decuzzi P and Ferrari M 2008 The receptor-mediated endocytosis of nonspherical particles *Biophys. J.* **94** 3790

[61] Decuzzi P, Pasqualini R, Arap W and Ferrari M 2009 Intravascular delivery of particulate systems: Does geometry really matter? *Pharmaceut Res* **26** 235 10.1007/s11095-008-9697-x

[62] Bardhan R, Lal S, Joshi A and Halas N J 2011 Theranostic nanoshells: From probe design to imaging and treatment of cancer *Accounts Chem Res* **44** 936

[63] Khlebtsov B, Zharov V, Melnikov A, Tuchin V and Khlebtsov N 2006 Optical amplification of

photothermal therapy with gold nanoparticles and nanoclusters *Nanotechnology* **17** 5167
[64] Huff T B, Tong L, Zhao Y, Hansen M N, Cheng J X and Wei A 2007 Hyperthermic effects of gold nanorods on tumor cells *Nanomed* **2 (1)** 125132
[65] Lukianova-Hleb E Y, Hanna E Y, Hafner J H and Lapotko D O 2010 Tunable plasmonic nanobubbles for cell theranostics *Nanotechnology* **21** 085102
[66] Chen C L, Kuo L R, Chang C L, Hwu Y K, Huang C K, Lee S Y, Chen K, Lin S J, Huang J D and Chen Y Y 2010 In situ real-time investigation of cancer cell photothermolysis mediated by excited gold nanorod surface plasmons *Biomaterials* **31** 4104
[67] Braun G B, Pallaoro A, Wu G, Missirlis D, Zasadzinski J A, Tirrell M and Reich N O 2009 Laser-activated gene silencing via gold nanoshellsirna conjugates *ACS Nano* **3** 2007
[68] Jelveh S and Chithrani D B 2011 Gold nanostructures as a platform for combinational therapy in future cancer therapeutics *Cancers* **3** 1081
[69] Jiang W, Kim B Y S, Rutka J T and Chan W C W 2008 Nanoparticle-mediated cellular response is size-dependent *Nature Nanotech* **3** 145
[70] Zhang S, Li J, Lykotrafitis G, Bao G and Suresh S 2008 Size-dependent endocytosis of nanoparticles *Adv Mater* **21 (4)** 419
[71] Gao H, Shi W and Freund L B 2005 Mechanics of receptor-mediated endocytosis *PNAS* **102 (27)** 9469
[72] Ungureanu C, Kroes R, Petersen W, Groothuis T A M, Ungureanu F, Janssen H, van Leeuwen F W B, Kooyman R P H, Manohar S and van Leeuwen T G 2011 Light interactions with gold nanorods and cells: Implications for photothermal nanotherapeutics *Nano Letters* **11** 1887
[73] Gonzlez M G, Liu X, Niessner R and Haischa C 2010 Strong size-dependent photoacoustic effect on gold nanoparticles by laser-induced nanobubbles *Appl Phys Lett* **96** 174104
[74] Liu C, Li Z and Zhang Z 2009 Mechanisms of laser nanoparticle-based techniques for gene transfectiona calculation study *J Biol Phys* **35** 175
[75] Akchurin G, Khlebtsov B, Akchurin G, Tuchin V, Zharov V and Khlebtsov N 2008 Gold nanoshell photomodification under a single-nanosecond laser pulse accompanied by color-shifting and bubble formation phenomena *Nanotechnology* **19** 015701
[76] Didychuk C L, Ephrat P, Chamson-Reig A, Jacques S L and Carson J J L 2009 Depth of photothermal conversion of gold nanorods embedded in a tissue-like phantom *Nanotechnology* **20** 195102
[77] Link S and El-Sayed M 2000 Spectroscopic determination of the melting energy of a gold nanorod *J Chem Phys* **114** 2362
[78] Qi W and Wang M 2004 Size and shape dependent melting temperature of metallic nanoparticles *Mat Chem Phys* **88** 280284
[79] Alekseeva A V, Bogatyrev V A, Dykman L A, Khlebtsov B N, Trachuk L A, Melnikov A G and Khlebtsov N G 2005 Preparation and optical scattering characterization of gold nanorods and their application to a dot-immunogold assay *Appl. Opt.* **44** 6285
[80] Jana N R, Gearheart L and Murphy C J 2001 Seed-mediated growth approach for shape-controlled synthesis of spheroidal and rod-like gold nanoparticles using a surfactant template *Adv. Mater.* **13** 1389
[81] Pérez-Juste J, Liz-Marzán L M, Carnie S, Chan D Y C and Mulvaney P 2004 Electric-field-directed growth of gold nanorods in aqueous surfactant solutions *Adv. Func. Mater.* **14** 571
[82] Xia Y, Xiong Y, Lim B and Skrabalak S E 2009 Shape-controlled synthesis of metal nanocrystals: Simple chemistry meets complex physics? *Angew. Chem. Int. Ed.* **48** 60
[83] Grzelczak M, Prez-Juste J, Mulvaney P and Liz-Marzán L M 2008 Shape control in gold nanoparticle synthesis *Chem. Soc. Rev.* **37** 1783
[84] Brioude A, Jiang X C and Pileni M P 2005 Optical properties of gold nanorods:? dda simulations supported by experiments *J. Phys. Chem. B* **109** 13138
[85] Rayavarapu R G, Petersen W, Chin P, Janssen H, van Leeuwen F W B, Manohar S and van Leeuwen T G 2010 In vitro toxicity studies of polymer-coated gold nanorods *Nanotechnology* **21**

145101

[86] Sharma V, Park K and Srinivasarao M 2009 Shape separation of gold nanorods using centrifugation *Proc. Natl. Acad. Sci.* **106** 4981

[87] Kirpotin D B, Drummond D C, Shao Y, M Refaat Shalaby and K H, Nielsen U B, Marks J D, Benz C C and Park J W 2006 Antibody targeting of long-circulating lipidic nanoparticles does not increase tumor localization but does increase internalization in animal models *Cancer Res* **66**

[88] KJain R 2005 Normalization of tumor vasculature: An emerging concept in antiangiogenic therapy *Science* **307** 58

[89] Sonveaux P 2008 Provascular strategy: Targeting functional adaptations of mature blood vessels in tumors to selectively influence the tumor vascular reactivity and improve cancer treatment *Radiother Oncol* **86 (3)** 300

[90] Kong G, Braun R D and Dewhirst M W 2000 Hyperthermia enables tumor-specific nanoparticle delivery: Effect of particle size *Cancer Res* **60** 4440

[91] Li L, ten Hagen T L, Schipper D, Wijnberg T M, van Rhoon G C, Eggermont A M, Lindner L H and Koning G A 2010 Triggered content release from optimized stealth thermosensitive liposomes using mild hyperthermia *J Controlled Release* **143** 274

[92] Jain R K 1990 Physiological barriers to delivery of monoclonal antibodies and other macromolecules in tumors *Cancer Res* **50** 814

[93] Kessentini S, Barchiesi D, Grosges T and de la Chapelle M L 2011 Selective and collaborative optimization methods for plasmonics: A comparison *PIERS Online* **7(3)** 291